Organic & Biomolecular Chemistry

ROYAL SOCIETY OF CHEMISTRY

COMMUNICATION

View Article Online
View Journal | View Issue

Open Access Article. Published on 26 November 2025. Downloaded on 1/22/2026 10:11:49 AM.
This article is licensed under a Creative Commons Attribution 3.0 Unported Licence.

Check for updates

Cite this: *Org. Biomol. Chem.*, 2026, **24**, 87

Received 3rd November 2025,
Accepted 25th November 2025

DOI: 10.1039/d5ob01728a

rsc.li/obc

Electrochemically-generated ferricyanide enables thiol–ene capture of protein–protein binding

André Campaniço, Denise Sommer, Christopher Batchelor-McAuley * and Joanna F. McGouran *

Due to its efficiency, selectivity and biocompatibility, the thiol–ene coupling has demonstrated its potential for protein labelling. Here, we report the electrochemical thiol–ene activation to capture protein–protein binding events. *In situ* electrochemical generation of Fe(III) was used as the first example of an electrochemically generated thiol–ene protein–protein labelling reaction.

Introduction

The thiol–ene coupling, first described in 1905, comprises the coupling of a carbon–carbon double bond and a thiol to form a thioether.[1,2] The specificity of this reaction for thiol moieties and mild reaction conditions makes it particularly well-suited for the labelling of thiols present in free cysteine residues in proteins. The low relative abundance of cysteine residues leads to them being attractive targets for labelling assays, as they make up approximately 2% of residues within the human proteome, with many located in the active site of proteins.[3] As such, the thiol–ene reaction has been utilised for site-specific protein labelling with both proteins and small molecule tags.[4,5] Furthermore, this strategy has been shown to capture protein–protein binding events in which an alkene on one protein is brought into close proximity to a free cysteine residue on its binding partner.[6] This approach has been recently advanced through the use of a photochemically-triggerable synthetic process. Control of the timing of the binding has the potential to not only improve the selective detection of active enzymes but to also enable the development of time-resolved kinetic assays.

As a controlling mechanism, electrochemistry has been employed in a range of bioanalytical systems. As an example, the use of electrochemiluminescence (ECL) has led to the development of high sensitivity immunoassays, which are capable of outperforming traditional ELISA systems.[7] These ECL-immmunoassays utilise the ability to turn the luminescent signal 'on' and 'off' to improve the systems background-to-noise ratio. However, beyond analysis, electrochemistry has played a significant role in chemical synthesis for over a century.[8,9] This approach enables precise modulation of reaction conditions through adjustment of the electrode potential, mild reaction conditions, scalability, and *in situ* generation of reactive intermediates,[10,11] thus making electrochemistry an attractive field for biological applications. Within chemical biology, the use of electrochemistry has been previously reported in bioconjugation reactions, with site-specific labelling of residues like tyrosine or tryptophan.[9,12,13] More broadly, the use of thiol–ene chemistry has found wide use in organic chemistry, where the reaction is routinely undertaken with both thermal and photochemical radical initiators.[14,15] Given that the reaction proceeds *via* the oxidation of the thiol to the corresponding thiyl radical, electrochemistry would appear to be ideally suited to bring about the reaction. However, reports of the use of electrochemistry to initiate the thiol–ene reaction are surprisingly sparse in the literature. In an electrochemistry context, it appears that the thiol–ene reaction conditions need to be markedly altered for significant yields to be attained, often avoiding the hydrogen abstraction propagation step. For example, the work by Lei *et al.*[16] required further oxidation of the carbon radical intermediate and addition of a nucleophile to trap the electrochemically-generated carbocation intermediate. Redox initiation of the thiol–ene reaction seems to often favour the formation of the disulfide product as opposed to the thioether.[17] Li *et al.*[18] have partially circumvented this issue by electrochemically utilising a thin-layer cell so that the disulfide product can be reduced and recycled. However, in the present work, we demonstrate how the use of a sterically-hindered thiol group allows this disulfide formation to be essentially blocked, ensuring the thiol–ene reaction is able to proceed even under mild redox initiation conditions and can be triggered electrochemically.

A model system consisting of a C-terminally modified ubiquitin, bearing an alkene, and the cysteine-containing deubiquitinating enzyme OTUB1 (Ovarian Tumor Domain-Containing Ubiquitin Aldehyde-Binding Protein 1) have been

School of Chemistry, Trinity College Dublin, Dublin 2, Ireland.
E-mail: jmcgoura@tcd.ie, chris.mcauley@tcd.ie

Open Access Article. Published on 26 November 2025. Downloaded on 1/22/2026 10:11:49 AM.
This article is licensed under a Creative Commons Attribution 3.0 Unported Licence.

chosen for this proof-of-principle study. Ubiquitin activity-based probes (ABPs) are well-established chemical tools to label active deubiquitinases (DUBs), utilising ubiquitin as a recognition motif for precise positioning of a reactive "warhead" in the DUB active site. Substitution of the scissile ubiquitin C-terminal isopeptide bond with a reactive moiety enables covalent capture of the catalytic cysteine thiol.[19,20] Warhead variation has been previously studied and optimised for optimal alignment with the active-site thiol.[21] Probe **1**, bearing an alkene warhead, was previously shown to form a covalent adduct with target DUBs upon photochemical and redox activation. Furthermore, a C91S active site point mutant of OTUB1 showed no significant adduct formation with probe **1**, demonstrating the selective labelling of the active site thiol of OTUB1 by probe **1**.[17,22] Based on analogy of probe **1** with previous ubiquitin probe generations, we propose that covalent capture of the deubiquitinating enzyme active site cysteine occurs at the C2 position of probe **1** (Fig. 1).[23] Ubiquitination is a fundamental post-translational modification that regulates protein function, localisation, and degradation within the cell.[24,25] Removal of ubiquitin is mediated by DUBs, a family of about 100 proteins classified into seven subfamilies, six of which function as cysteine proteases.[26,27] Dysregulation of DUB activity has been associated with pathological conditions, including cancer,[28,29] neurodegenerative diseases,[30] and inflammatory disorders.[31] More specifically, OTUB1 has been linked to several cancer types, including lung cancer, ovarian cancer and breast cancer.[32–34] Ubiquitin-based probes have proven to be powerful tools for investigating DUB function, taking advantage of their active-site cysteine for selective labelling.[35,36] Herein, we report the use of electrochemically-generated ferricyanide in the activation of thiol–ene coupling between alkene-bearing ubiquitin probe **1** and the DUB OTUB1 (Fig. 1). Potassium ferricyanide was selected as the chemical initiator. This species is a weak inorganic oxidising agent and is known to be able to oxidise free thiols.[37] This proof-of-concept work demonstrates how the protein binding event can be triggered electrochemically and has future potential to be applied in automated systems, comparable to those used in ECL-immunoassays. However, here in contrast to the ECL-immunoassay strategy, instead of using a voltage difference as a highly sensitive method to transduce an analytical signal, the present work demonstrates that, in principle, electrochemical initiation can be used to synthetically trigger covalent capture of a protein–protein binding event.

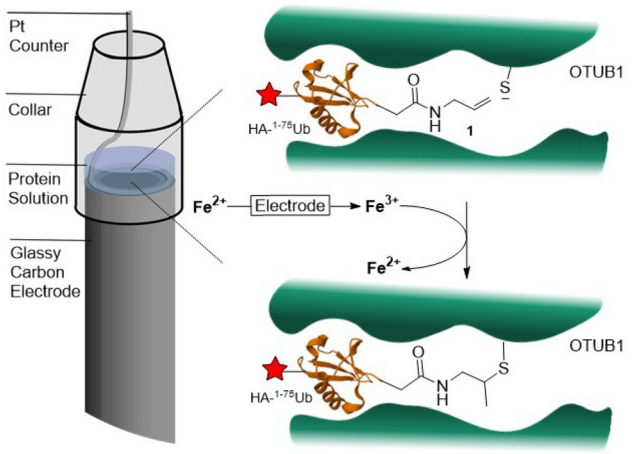

Fig. 1 Proposed mechanism for the activation of thiol–ene in the labelling of deubiquitinases, with *in situ* electrochemical generation of Fe(III).

Results and discussion

This work starts by evidencing that ferricyanide can be used to effectively initiate the covalent capture of a protein–protein binding event through a thio–ene reaction process. Subsequent to this, the work moves to demonstrate how a simplified two-electrode setup can be used to effectively generate the required oxidising agent *in situ* and initiate protein–protein binding.

The protein binding event chosen was an alkene-functionalized ubiquitin-probe with a hemagglutinin (HA) tag (HA-$^{1-75}$Ub-alkene probe **1**) and the deubiquitinating enzyme OTUB1. Probe **1** bears an alkene group in place of the native scissile isopeptide bond at the C-terminus of ubiquitin, positioning the alkene in close proximity to the DUB active-site thiol upon protein–protein binding (Fig. 1).[6] Previous work with probe **1** has shown that labelling activation can be carried out using UV- and visible light-dependent initiators, and chemical initiators, such as manganese(III) acetate. The use of chemical initiators enables thiol–ene coupling in protein systems in which the alkene and the thiol are brought into close proximity. Similar redox initiation in small molecule models with no induced proximity was previously demonstrated to favour disulfide formation.[17] However, in the case of protein–protein binding, this disulfide bond formation becomes sterically blocked, enabling the thiol–ene reaction to proceed, even under conditions where for small molecule systems, the resulting product is the disulfide as opposed to the thioether.

First, to ascertain the capacity of potassium ferricyanide to trigger thiol–ene labelling between probe **1** and OTUB1, the proteins were incubated for 1 hour with potassium ferricyanide and separately with potassium ferrocyanide, to provide a direct comparison. Here, the cyanide complex has been selected for use on the basis of stability of the ligands, ensuring that the likely dominant pathway for interaction is *via* electron transfer as opposed to, for example, binding of a thiol to the iron centre. The stability constants for ferro- and ferricyanide are reported to be $\log k$ = 35.4 and 43.6 respectively,[38] indicating that only trace quantities of the non-complexed iron species are expected to be present in the solution. On the basis of the proposed mechanism for redox thiol–ene activation (SI Fig. S1), it was expected that only potassium ferricyanide (Fe^{3+}) would be capable of initiating this reaction. A photo-initiated thiol–ene reaction using a mixture of 2,2-dimethoxy-2-phenyla-

 This journal is © The Royal Society of Chemistry 2026

Open Access Article. Published on 26 November 2025. Downloaded on 1/22/2026 10:11:49 AM.
This article is licensed under a Creative Commons Attribution 3.0 Unported Licence.

cetophenone (DPAP) and methoxyacetophenone (MAP) was used as positive control for the experiment (Fig. 2, lane 4) and a sample with no initiator was used as negative control (Fig. 2, lane 3). Following SDS-PAGE analysis and Western Blot visualisation, labelling was observed with potassium ferricyanide (Fig. 2, lane 5), through formation of a new band with a molecular weight corresponding to the expected OTUB1-Probe **1** covalent adduct (Fig. 2, blue arrow), while unreacted probe **1** was observed at a lower molecular weight (Fig. 2, white arrow). Due to protein denaturation prior to gel loading, only covalent protein–probe adducts can be observed. As expected, potassium ferrocyanide did not activate the coupling between probe **1** and OTUB1 (Fig. 2, lane 6). This lack of coupling in the presence of the ferrocyanide reflects the inability of the species to oxidise the thiol substrate and create a covalent adduct.

To optimise potassium ferricyanide as a thiol–ene chemical initiator, probe **1** and OTUB1 were incubated with potassium ferricyanide at different incubation times and labelling was analysed with SDS-PAGE and visualised using anti-HA Western Blot (Fig. 3). Different incubation times were analysed and it was observed that, after 5 minutes of incubation, OTUB1 labelling displayed an intensity comparable with the positive control (Fig. 3, lane 4 *vs.* 6). Longer incubation times improved labelling intensity and optimal incubation time was determined to be 60 minutes (Fig. 3, lane 9). The result obtained is similar to previous assays with manganese(III) acetate, a redox initiator previously used in this thiol–ene coupling.[17]

Following time optimisation, we next turned our attention to optimisation of concentrations of potassium ferricyanide (Fig. 4). Once again, OTUB1 labelling was successful, with all concentrations over 50 μM rendering significant labelling (Fig. 4, lanes 7–10). Furthermore, similar labelling intensities were accomplished with 50 μM of potassium ferricyanide and

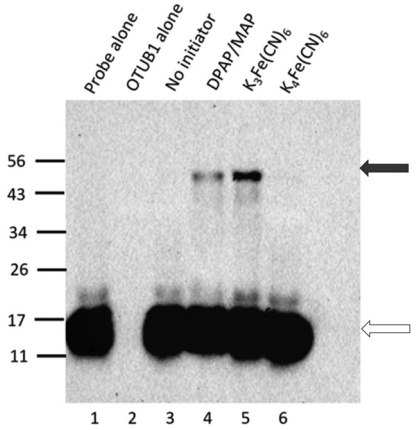

Fig. 2 Comparative analysis of Fe(III) and Fe(II) in the thiol–ene labelling of OTUB1 (1 μg) with probe **1** (2 μg). Assay visualised by anti-HA Western Blotting. Samples were incubated for 90 min at 37 °C, prior to initiator addition. A mixture of DPAP and MAP was used as positive control (lane 4). Potassium ferricyanide (500 μM) and potassium ferrocyanide (500 μM) were added to lanes 5 and 6, respectively, which were incubated at 37 °C for 60 min.

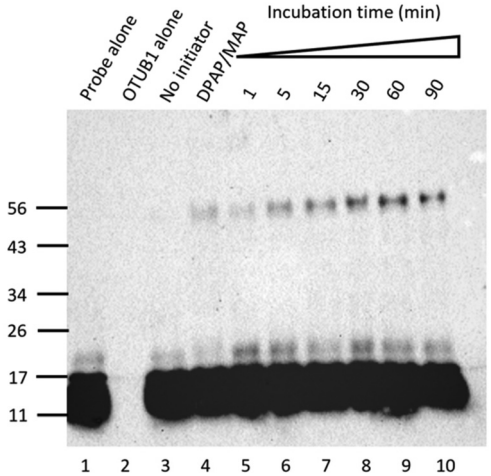

Fig. 3 Incubation time optimisation for the labelling of OTUB1 (1 μg) with probe **1** (2 μg), using Fe(III) as chemical initiator. Assay visualised by anti-HA Western Blotting. Samples were incubated for 90 min at 37 °C, prior to initiator addition. A mixture of DPAP and MAP was used as positive control (lane 4). Potassium ferricyanide (500 μM) was added to lanes 5–10, which were incubated at 37 °C for varying periods of time.

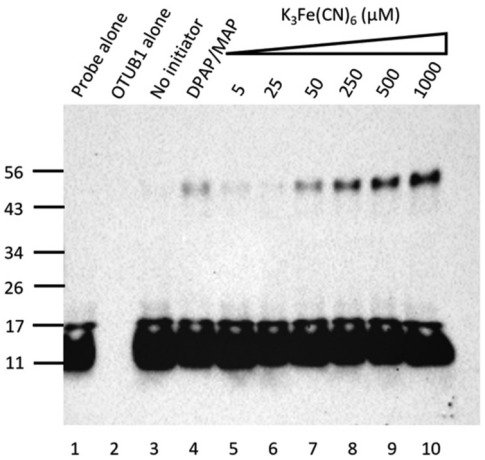

Fig. 4 Optimisation of Fe(III) concentration for the thiol–ene labelling of OTUB1 (1 μg) with probe **1** (2 μg). Assay visualised by anti-HA Western Blotting. Samples were incubated for 90 min at 37 °C, prior to initiator addition. A mixture of DPAP and MAP was used as positive control (lane 4). Varying concentrations of potassium ferricyanide were added to lanes 5–10, which were incubated at 37 °C for 60 min.

500 μM of DPAP/MAP (the positive control) (Fig. 4, lanes 4 *vs.* 7), albeit with a longer incubation time, which attests the efficiency of redox initiation in triggering this thiol–ene coupling. Optimal potassium ferricyanide concentrations were determined to range between 250 μM and 1 mM (Fig. 4, lanes 8–10).

Following confirmation of potassium ferricyanide's suitability as a thiol–ene redox initiator for protein labelling, an electrochemical setup for the *in situ* conversion of ferrocyanide into ferricyanide, in solution with probe **1** and OTUB1, was developed. A schematic of this experimental set up is also

Open Access Article. Published on 26 November 2025. Downloaded on 1/22/2026 10:11:49 AM.
This article is licensed under a Creative Commons Attribution 3.0 Unported Licence.

shown in Fig. 1. Considering the small volumes required for this assay, a two-electrode set-up was optimised for the *in situ* conversion of Fe(II) into Fe(III) (SI section 2). In this setup, a platinum wire counter electrode was used. Platinum is a good electrocatalytic material for both hydrogen evolution and oxygen reduction. Hence, given the buffering capacity of the solution, it is assumed that the counter electrode reaction will correspond to the formation of either hydrogen, or the reduction of oxygen to water, both of these irreversible reaction processes are unlikely to interfere with the ferricyanide product formed at the working substrate. Furthermore, due to the used cell geometry and timescale of the electrolysis, the working and counter electrodes are not in diffusional contact during the course of the electrosynthesis. Consequently, the amount of Fe(III) generated in the system can be simply and accurately determined by measuring the current passed through the system. Herein, for the reported electrochemically-generated concentrations of ferricyanide, it is assumed that the process occurs with complete faradaic efficiency, hence the reported values likely represent a marginal over-estimation of the total produced Fe(III) concentration. However, under this assumption, the amount of charge required for generation of an initial concentration of Fe(III) of 500 μM was calculated using Faraday's law and the known sample volume (150 μC, see Table S1 for more details) and samples were incubated at different incubation times with electrochemically-generated Fe (III) (SI Fig. S3). Though this first preliminary assay lacked efficiency, labelling was still observed after 30, 60 and 90 min of incubation. Pleasingly, apart from demonstrating that thiol–ene protein labelling is possible using electrochemical initiation, the optimal incubation time for this assay was lowered to 30 min. Following this result, a new assay was envisioned to further optimise the use of electrochemically-generated ferricyanide in OTUB1 labelling. The extent of electrolysis at the working electrode was varied, with control of the total charge passed. The experimental oxidative charge was in the range of 7.5 to 1500 μC, leading to the controlled generation of ferricyanide concentrations between 2.5 and 500 μM (SI Table S1). Following Fe(III) *in situ* generation with probe **1** and OTUB1, the system was further incubated with the electrochemically-converted initiator for 30 min (Fig. 5). Protein labelling was observed above background levels at concentrations 25 μM and 50 μM (Fig. 5, Lanes 7 and 8). The optimal concentration was deemed to be 50 μM. Unlike previous assays with ferricyanide, higher concentrations (250 μM and 500 μM) did not afford stronger labelling. However, the lack of protein labelling at higher concentrations of generated ferricyanide may be explained by altered initial Fe(II) concentrations used in the electrochemical cell (1 mM *vs.* 10 mM). To generate the higher ferricyanide concentrations, higher initial concentrations of ferrocyanide were used to ensure significant Fe(III) production over a reasonable time during electrolysis. The interfacial reaction for the conversion of Fe(II) to Fe(III) is controlled by both the mass-transport of the material to the electrode interface and the concentration of the reagent (Fe(II)); consequently, for these higher Fe(III) concentrations (250 μM and 500 μM), solutions initially containing 10 mM Fe(II) were used and hence, after electrochemical conversion, a higher concentration of non-converted Fe(II) species remained in solution. The presence of higher concentrations of the reduced species will lead to a decrease in the thermodynamic driving force for the solution phase reaction involving the ferricyanide oxidation of the thiolate to the thiyl radical. Assuming that this initial oxidation of the thiol is to some extent under thermodynamic control then this change in the driving force for the homogenous reaction as a function of the ratio of the Fe(II) to Fe(III) will be described by the Nernst equation. Hence, for the 250 μM and 500 μM experiments, the ratio of the Fe(II) to Fe(III) concentrations is the same as the 25 μM and 50 μM experiments. This result tentatively indicates that the redox initiation of the thiol–ene reaction is sensitive to the solution phase redox potential (*i.e.* the ratio of the reduced and oxidised species) and not simply the total concentration of the Fe(III) in the solution. This decrease in the labelling at higher concentrations, also provides indirect evidence that the counter electrode reaction is not influential in initiating the protein/protein binding. Still, significant protein labelling was observed at lower concentrations, suggesting that though higher concentrations may be advantageous, they are not required. A concentration of generated Fe(III) of 50 μM is enough to trigger thiol–ene protein labelling. This result shows that it is possible to electrochemically-generate a thiol–ene initiator *in situ* and that this process can be used in thiol–ene protein labelling, requiring low concentrations of initiator and lowering the required incubation time.

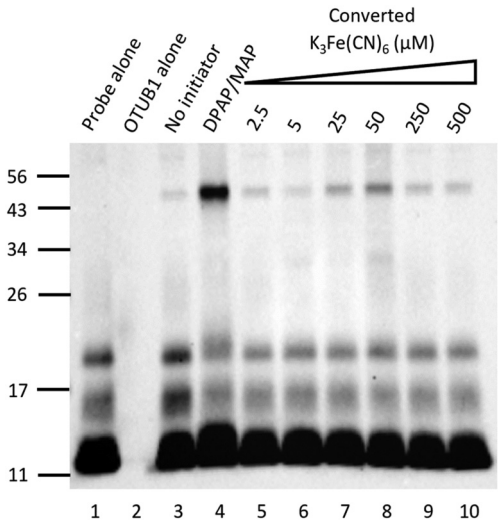

Fig. 5 Optimisation of concentration of electrochemically-generated Fe(III) for the thiol–ene labelling of OTUB1 (1 μg) with probe **1** (2 μg). Assay visualised by anti-HA Western Blotting. Samples were incubated for 90 min at 37 °C, prior to initiator addition. A mixture of DPAP and MAP was used as positive control (lane 4). Lanes 5–10 were treated with potassium ferrocyanide (Lanes 5–8: 1 mM; Lanes 9–10: 10 mM) and sodium chloride (50 mM). Varying charges were applied to generate concentrations of ferricyanide 2.5–500 μM. Lanes 5–10 were then incubated at 37 °C for 30 min.

Open Access Article. Published on 26 November 2025. Downloaded on 1/22/2026 10:11:49 AM.
This article is licensed under a Creative Commons Attribution 3.0 Unported Licence.

Conclusions

We have demonstrated that *in situ* electrochemical generation of ferricyanide can be used in thiol–ene protein labelling to covalently capture protein–protein binding events. To the best of our knowledge, this is the first time a redox initiator was electrochemically-generated *in situ* to activate thiol–ene labelling between two proteins. This technique holds potential application in the development of automated immunoassays based on triggering protein–protein adduct formation, not using a UV light source but *via* the occurrence of an electrochemical reaction. Further, this is one of the first examples where the thiol–ene chemistry can be initiated electrochemically using a redox mediator and without recourse to the use of nucleophilic additives or significant alteration of the chemical conditions. Potassium ferricyanide is an efficient chemical initiator for thiol–ene labelling of OTUB1, which likely reflects the fact that formation of the disulfide product is essentially completely blocked. Potassium ferrocyanide was also tested and no protein labelling was observed; this null result is important in evidencing that the presence of the ferricyanide leads to covalent bond formation between the proteins. Following these findings, an electrochemical setup was developed for this system, with adaptations for the small volumes used in the labelling assay. Electrochemical conversion of ferrocyanide into ferricyanide was calculated to generate precise Fe(III) concentrations and these were used to initiate thiol–ene coupling between probe **1** and OTUB1. *In situ* electrochemical generation of the Fe(III) initiator resulted in protein labelling, at low concentrations and lower incubation times than those required in the corresponding chemical assays. This exciting proof-of-concept study paves the way for further exploration of the potential of thiol–ene labelling in electrochemical settings.

Author contributions

Conceptualisation, J. F. M. and C. B.M.; funding acquisition, J. F. M. and C. B.M.; methodology, A. C., J. F. M. and C. B.M.; experimental data collection and analysis, A. C. and D. S.; supervision, J. F. M. and C. B.M.; project administration, J. F. M. and C. B.M.; writing, A. C., J. F. M. and C. B.M.

Conflicts of interest

There are no conflicts to declare.

Data availability

Supplementary information: experimental, supplementary electrochemistry experimental data, supplementary Western Blots. See DOI: https://doi.org/10.1039/d5ob01728a.

Acknowledgements

This project was funded by the Higher Education Authority (HEA), project 213057 (J.F.M.) and Research Ireland, 22/FFP-P/11234 (J.F.M.)

References

1 T. Posner, *Ber. Dtsch. Chem. Ges.*, 1905, **38**, 646–657.
2 C. E. Hoyle and C. N. Bowman, *Angew. Chem., Int. Ed.*, 2010, **49**, 1540–1573.
3 A. Miseta and P. Csutora, *Mol. Biol. Evol.*, 2000, **17**, 1232–1239.
4 M. D. Nolan and E. M. Scanlan, *Front. Chem.*, 2020, **8**, 1–21.
5 E. M. Valkevich, R. G. Guenette, N. A. Sanchez, Y.-c. Chen, Y. Ge and E. R. Strieter, *J. Am. Chem. Soc.*, 2012, **134**, 6916–6919.
6 N. C. Taylor, G. Hessman, H. B. Kramer and J. F. McGouran, *Chem. Sci.*, 2020, **11**, 2967–2972.
7 L. Li, Y. Chen and J.-J. Zhu, *Anal. Chem.*, 2017, **89**, 358–371.
8 M. Faraday, *Ann. Phys.*, 1834, **109**, 433–451.
9 C. Loynd, S. J. Singha Roy, V. J. Ovalle, S. E. Canarelli, A. Mondal, D. Jewel, E. D. Ficaretta, E. Weerapana and A. Chatterjee, *Nat. Chem.*, 2024, **16**, 389–397.
10 E. J. Horn, B. R. Rosen and P. S. Baran, *ACS Cent. Sci.*, 2016, **2**, 302–308.
11 M. Yan, Y. Kawamata and P. S. Baran, *Chem. Rev.*, 2017, **117**, 13230–13319.
12 S. Depienne, D. Alvarez-Dorta, M. Croyal, R. C. T. Temgoua, C. Charlier, D. Deniaud, M. Mével, M. Boujtita and S. G. Gouin, *Chem. Sci.*, 2021, **12**, 15374–15381.
13 S. Depienne, M. Bouzelha, E. Courtois, K. Pavageau, P.-A. Lalys, M. Marchand, D. Alvarez-Dorta, S. Nedellec, L. Marín-Fernández, C. Grandjean, M. Boujtita, D. Deniaud, M. Mével and S. G. Gouin, *Nat. Commun.*, 2023, **14**, 5122.
14 J. T. McLean, A. Benny, M. D. Nolan, G. Swinand and E. M. Scanlan, *Chem. Soc. Rev.*, 2021, **50**, 10857–10894.
15 N. Ostrovitsa, C. Williams, K. Raabe, J. T. McLean, M. Muttenthaler and E. M. Scanlan, *Chem. – Eur. J.*, 2025, **31**, e202501372.
16 Y. Yuan, Y. Chen, S. Tang, Z. Huang and A. Lei, *Sci. Adv.*, 2018, **4**, eaat5312.
17 A. Campaniço, M. Baran, A. G. Bowie, D. B. Longley, T. Harrison and J. F. McGouran, *Commun. Chem.*, 2025, **8**, 25.
18 D. Li, S. Li, C. Peng, L. Lu, S. Wang, P. Wang, Y.-H. Chen, H. Cong and A. Lei, *Chem. Sci.*, 2019, **10**, 2791–2795.
19 R. Ekkebus, S. I. van Kasteren, Y. Kulathu, A. Scholten, I. Berlin, P. P. Geurink, A. de Jong, S. Goerdayal, J. Neefjes, A. J. Heck, D. Komander and H. Ovaa, *J. Am. Chem. Soc.*, 2013, **135**, 2867–2870.
20 S. Sommer, N. D. Weikart, U. Linne and H. D. Mootz, *Bioorg. Med. Chem.*, 2013, **21**, 2511–2517.

Open Access Article. Published on 26 November 2025. Downloaded on 1/22/2026 10:11:49 AM.
This article is licensed under a Creative Commons Attribution 3.0 Unported Licence.

21 E. Mons, R. Q. Kim, B. R. van Doodewaerd, P. A. van Veelen, M. P. C. Mulder and H. Ovaa, *J. Am. Chem. Soc.*, 2021, **143**, 6423–6433.
22 N. C. Taylor and J. F. McGouran, *Org. Biomol. Chem.*, 2021, **19**, 2177–2181.
23 A. Borodovsky, H. Ovaa, N. Kolli, T. Gan-Erdene, K. D. Wilkinson, H. L. Ploegh and B. M. Kessler, *Chem. Biol.*, 2002, **9**, 1149–1159.
24 R. Yau and M. Rape, *Nat. Cell Biol.*, 2016, **18**, 579–586.
25 P. P. Di Fiore, S. Polo and K. Hofmann, *Nat. Rev. Mol. Cell Biol.*, 2003, **4**, 491–497.
26 M. J. Clague, S. Urbé and D. Komander, *Nat. Rev. Mol. Cell Biol.*, 2019, **20**, 338–352.
27 S. A. Abdul Rehman, Y. A. Kristariyanto, S. Y. Choi, P. J. Nkosi, S. Weidlich, K. Labib, K. Hofmann and Y. Kulathu, *Mol. Cell*, 2016, **63**, 146–155.
28 M. Mondal, F. Cao, D. Conole, H. W. Auner and E. W. Tate, *RSC Chem. Biol.*, 2024, **5**, 439–446.
29 S. Javaid, S. Zadi, M. Awais, A.-t. Wahab, H. Zafar, I. Maslennikov and M. I. Choudhary, *RSC Adv.*, 2024, **14**, 33080–33093.
30 M. Boselli, B. H. Lee, J. Robert, M. A. Prado, S. W. Min, C. Cheng, M. C. Silva, C. Seong, S. Elsasser, K. M. Hatle, T. C. Gahman, S. P. Gygi, S. J. Haggarty, L. Gan, R. W. King and D. Finley, *J. Biol. Chem.*, 2017, **292**, 19209–19225.
31 B. Wu, L. Qiang, Y. Zhang, Y. Fu, M. Zhao, Z. Lei, Z. Lu, Y.-G. Wei, H. Dai, Y. Ge, M. Liu, X. Zhou, Z. Peng, H. Li, C.-P. Cui, J. Wang, H. Zheng, C. H. Liu and L. Zhang, *Cell. Mol. Immunol.*, 2022, **19**, 276–289.
32 D. Zhu, R. Xu, X. Huang, Z. Tang, Y. Tian, J. Zhang and X. Zheng, *Cell Death Differ.*, 2021, **28**, 1773–1789.
33 Y. Wang, X. Zhou, M. Xu, W. Weng, Q. Zhang, Y. Yang, P. Wei and X. Du, *Oncotarget*, 2016, **7**, 36681–36697.
34 M. F. Baietti, M. Simicek, L. Abbasi Asbagh, E. Radaelli, S. Lievens, J. Crowther, M. Steklov, V. N. Aushev, D. Martínez García, J. Tavernier and A. A. Sablina, *EMBO Mol. Med.*, 2016, **8**, 288–303.
35 J. Farnung, K. A. Tolmachova and J. W. Bode, *Chem. Sci.*, 2023, **14**, 121–129.
36 X. Sui, Y. Wang, Y.-X. Du, L.-J. Liang, Q. Zheng, Y.-M. Li and L. Liu, *Chem. Sci.*, 2020, **11**, 12633–12646.
37 K. B. Wiberg, H. Maltz and M. Okano, *Inorg. Chem.*, 1968, **7**, 830–831.
38 D. R. Burgess, *NIST SRD 46, Critically Selected Stability Constants of Metal Complexes: Version 8.0 for Windows*, National Institute of Standards and Technology, 2004.

 This journal is © The Royal Society of Chemistry 2026